

191041. Polarimetric Properties of Ice Cloud Particles at S band

Valery Melnikov

University of Oklahoma, CIMMS and NOAA/NSSL, Norman, OK

1. Introduction

Radar remote sensing of clouds is an important source of information on cloud microphysics. The empirical relations between particles' sizes, shapes, and densities have been used to calculate radar reflectivity, Z , differential reflectivity, Z_{DR} , and the specific differential phase, K_{dp} at cm-wavelengths (e.g., Vivekanandan et al. 1991, 1994; Matrosov et al. 1991, 1996). One more measurable parameter, i.e., the copolar correlation coefficient ρ_{hv} has not been considered. In calculation of Z , Z_{DR} , and K_{dp} it is usually assumed that cloud particles are oriented horizontally. The latter assumption is a serious limitation because cloud particles flatter and tumble in air that alters their polarimetric parameters from those calculated for horizontal orientation. We address this issue in this paper in considerations of Z_{DR} and ρ_{hv} .

Roughly, cloud particles can be represented by two shapes: 1) oblate spheroids, e.g., plates and dendrites, and 2) prolate spheroids, e.g., needles and columns. Radar observations show that Z_{DR} in clouds spread an interval from 0 to 10 dB and exhibit anti-correlation with the copolar correlation coefficient, ρ_{hv} (e.g., Melnikov et al. 2011). Hall et al. 1984, Illingworth et al. 1987, Hogan et al. .

(2002) showed that thin plates can produce Z_{DR} as high as 10 dB if they are horizontally oriented and radar employs the alternate polarization configuration. Z_{DR} and ρ_{hv} for plates and columns are analyzed below to distinguish between these types of particles with a polarimetric S band radar with the simultaneous transmission configuration. Experimental data have been collected with the WSR-88D KOUN situated in Norman, OK, USA.

2. Z_{DR} and ρ_{hv} of ice spheroids

We consider herein radar data collected in nonprecipitating clouds at subfreezing temperatures. Z_{DR} in such clouds are positive that indicates that cloud particles are non-spherical and have preferable horizontal orientations. Herein we consider two shapes of ice particles: plate-like and needle-like (columnar) ones. Geometry of the scattering particles and incident waves are sketched in Fig. 1. The direction of propagation of radio waves is determined by vector \mathbf{k} that lies along the x -axis, i.e., horizontal sounding is considered. This case is a good approximation for antenna elevations less than 10° . Consider scattering by a spheroid with two principal semi axes a and b and the axis of rotation OO' . For these particles, $a \geq b$.

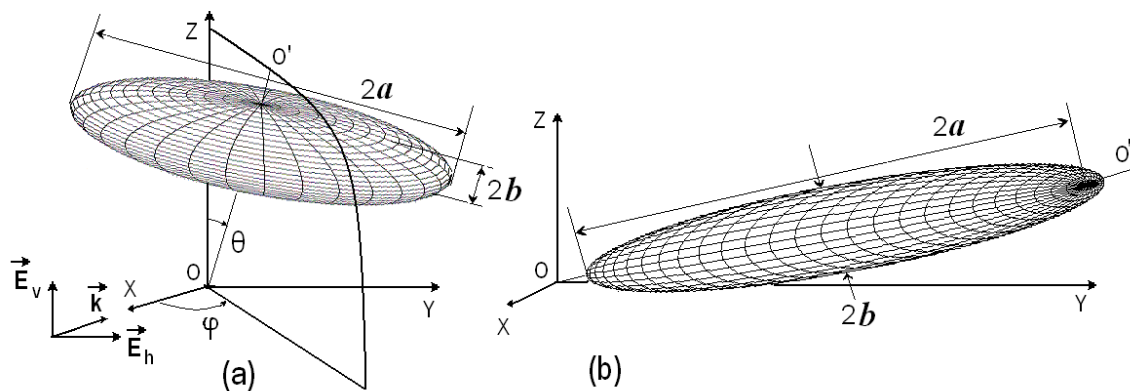


Fig. 1. Scattering geometry for (a) oblate and (b) prolate particles

The majority of polarimetric radars employ a polarimetric configuration with Simultaneous transmission and reception of Horizontally and Vertically polarized waves, i.e., the SHV mode. In such a configuration, signal paths in the two radar channels are different so the transmitted and received waves acquire phase differences ψ_t and ψ_r where subscripts stand for transmit and receive paths. A cloud of scatterers shifts the waves by the propagation differential phase φ_{dp} and differential phase upon scattering δ so that the measured phase shift is $\psi_{dp} = \psi_t + \psi_r + \varphi_{dp} + \delta = \psi_{sys} + \varphi_{dp} + \delta$ where $\psi_{sys} = \psi_t + \psi_r$ is usually called the system differential phase. To obtain the phases relevant to scattering particles, the system differential phase is subtracted from the measured phase, i.e., $\varphi_{dp} + \delta = \psi_{dp} - \psi_{sys}$.

In SNV mode, scattering of polarized radio-waves for CAN can be described by the following matrix equation:

$$\begin{pmatrix} E_{hr} \\ E_{vr} \end{pmatrix} = A \begin{pmatrix} S_{hh} & S_{hv} \\ S_{hv} & S_{vv} \end{pmatrix} B \begin{pmatrix} E_h \\ E_v \end{pmatrix}, \quad (1)$$

$$A = \begin{pmatrix} 1 \\ \exp[i(\psi_r + \frac{1}{2}\varphi_{dp})] \end{pmatrix},$$

$$B = \begin{pmatrix} 1 \\ \exp[i(\psi_t + \frac{1}{2}\varphi_{dp})] \end{pmatrix},$$

where S_{ij} are the scattering coefficients of the medium, $E_{h,v}$ are the amplitudes of the transmitted waves, and $E_{hr, vr}$ are the amplitudes of the received waves. In (1) range dependence and the radar constants are omitted without loss of generality because we are interested in Z_{DR} and ρ_{hv} that do not depend on those. The powers P_h , P_v and the correlation function for the signals are:

$$P_h = \langle |E_{hs}|^2 \rangle, \quad P_v = \langle |E_{vs}|^2 \rangle, \quad (2)$$

$$R_{hv} = \langle E_h^* E_v \rangle$$

where the brackets stand for ensemble averaging over all particles in the radar volume. Differential reflectivity Z_{DR} in dB and ρ_{hv} are

$$Z_{DR} = 10 \log_{10} \frac{P_h}{P_v}, \quad \rho_{hv} = \frac{|R_{vh}|}{(P_h P_v)^{1/2}}. \quad (3)$$

For a single scattering particle, the matrix coefficients are

$$S_{hh} = \alpha_a + \Delta\alpha \sin^2 \theta \sin^2 \varphi,$$

$$S_{vv} = \alpha_a + \Delta\alpha \cos^2 \theta,$$

$$S_{hv} = \Delta\alpha \sin \theta \cos \theta \sin \varphi,$$

$$\Delta\alpha = \alpha_b - \alpha_a, \quad (4)$$

where α_a and α_b are polarizabilities along a and b semi-axes (e.g., Bringi and Chandrasekar, 2001, Eq. (2.53)) and angles θ and φ are shown in Fig. 1. The calibration procedure takes care of difference in amplitudes E_h and E_v in (1) so we can assume that they are equal and omit them. We also neglect differential attenuation at S band in non-precipitating clouds. The differential phase due to propagation of S band radiation in nonprecipitating clouds can be neglected as well.

At S-band, cloud particles can be considered as Rayleigh scatterers and the polarizabilities for oblate spheroids are (e.g., Bohren and Huffman 1983, section 5.3):

$$\alpha_a = \frac{4}{3} \pi a^2 b \frac{\varepsilon - 1}{1 + L_a (\varepsilon - 1)}, \quad (5a)$$

$$\alpha_b = \frac{4}{3} \pi a^2 b \frac{\varepsilon - 1}{1 + L_b (\varepsilon - 1)}, \quad (5b)$$

$$L_a = \frac{g}{2e^2} \left(\frac{\pi}{2} - \tan^{-1} g \right), \quad L_b = 1 - 2L_a,$$

$$g = \left(\frac{1 - e^2}{e^2} \right)^{1/2}, \quad e^2 = 1 - (b/a)^2$$

where ε is dielectric permittivity of the scatterer relative to air. For a prolate scatterer,

$$L_a = \frac{1 - e^2}{e^2} \left(\frac{1}{2e} \ln \frac{1 + e}{1 - e} - 1 \right),$$

$$L_b = 0.5(1 - L_a), \quad (6)$$

$$e^2 = 1 - (b/a)^2, \quad a \geq b.$$

Substitution of (4) into (1) and (3) yields

$$P_h = |\alpha_a|^2 + 2 \operatorname{Re}(\alpha_a \Delta\alpha^*) \sin^2 \theta \sin^2 \varphi +$$

$$2 \operatorname{Re}(\alpha_a \Delta\alpha^* e^{-i\psi_t}) \sin \theta \cos \theta \sin \varphi +$$

$$2 |\Delta\alpha|^2 \sin^3 \theta \cos \theta \sin^3 \varphi \cos \psi_t +$$

$$|\Delta\alpha|^2 (\sin^4 \theta \sin^4 \varphi + \sin^2 \theta \cos^2 \theta \sin^2 \varphi) \quad (7a)$$

$$P_v = |\alpha_a|^2 + 2\text{Re}(\alpha\Delta\alpha^*)\cos^2\theta + 2\text{Re}(\alpha\Delta\alpha^*e^{i\psi_t})\sin\theta\cos\theta\sin\varphi + |\Delta\alpha|^2(\sin^2\theta\cos^2\theta\sin^2\varphi + \cos^4\theta + 2\sin\theta\cos\theta\sin\varphi\cos\psi_t) \quad (7b)$$

$$R_{hv} = [(|\alpha_a|^2 + \alpha\Delta\alpha^*\sin^2\theta\sin^2\varphi + \alpha^*\Delta\alpha\cos^2\theta)e^{i\psi_r} + 2\text{Re}(\alpha\Delta\alpha^*)\sin\theta\cos\theta\sin\varphi + |\Delta\alpha|^2(\sin^2\theta\cos^2\theta\sin^2\varphi + \cos^4\theta + 2\sin\theta\cos\theta\sin\varphi\cos\psi_t)]e^{i\psi_r} \quad (7c)$$

where $\text{Re}(x)$ stands for the real part of x . It is seen from (7) that the differential phase in receive ψ_r does not affect the received powers and consequently Z_{DR} .

It follows from (7a,b) that maximal Z_{DR} for oblate plate-like particles is 11.5 dB and is reached for $\psi_t = 0^\circ$, $\theta = 9.5^\circ$, and $\varphi = 90^\circ$. For the alternate transmission of polarized waves, maximal Z_{DR} is

$$Z_{DR(\text{max})} = 20\log(|\varepsilon|), \quad (8)$$

i.e., 10.0 dB. That is the SHV polarimetric configuration can produce larger maximal Z_{DR} due to depolarization of radiation by the cloud particles. Another distinction between the alternate and SHV configurations is dependence of ρ_{hv} upon the differential phase in transmit ψ_t . This dependence exists only for the SHV configuration.

For a horizontally oriented prolate scatterers ($\theta = 90^\circ$ in Fig. 1b), the maximal Z_{DR} is:

$$Z_{DR(\text{max})} = 20\log(0.5|\varepsilon + 1|). \quad (9)$$

For solid ice, the maximal Z_{DR} for a needle-like ice particle is 6.4 dB which is quite different from 11.5 dB obtained for plate-like ice particles. The maximal Z_{DR} of 6.4 dB for needle-like particles was obtained for a case for which the particle is oriented along the incident electric field. If the particles are oriented randomly in the horizontal plane, averaging (7) over φ yields

$$Z_{dr(\text{max})} = 10\log\left(1 + \frac{|\varepsilon - 1|}{2} + \frac{3|\varepsilon - 1|^2}{32}\right), \quad (10)$$

For needle-like ice particles, the maximal Z_{DR} is 4.0 dB. Comparing with maximal Z_{DR} of 10 dB for plate-like particles, we conclude that it is possible to distinguish these two types of shapes if measured Z_{DR} exceeds 4 dB. In such cases, plate-like particles contribute mostly to radar returns.

Maximal Z_{DR} (8) – (10) are for particles oriented in the horizontal plane. Cloud particles flatter and tumble in the air so that they should be characterized with distributions in θ and φ . For the uniform distribution in φ and independent distributions in size and orientation, the mean variables in (7) can be written as

$$P_h = \langle |\alpha_a|^2 \rangle + \text{Re}(\langle \alpha_a \Delta \alpha^* \rangle) J_1 + \frac{1}{8} \langle |\Delta \alpha|^2 \rangle (4J_1 - J_2) \quad (11a)$$

$$P_v = \langle |\alpha_a|^2 \rangle + 2\text{Re}(\langle \alpha_a \Delta \alpha^* \rangle) (1 - J_1) + \frac{1}{2} \langle |\Delta \alpha|^2 \rangle (2 - 3J_1 + J_2) \quad (11b)$$

$$R_{hv} = \{[\langle |\alpha_a|^2 \rangle + \frac{1}{2} \langle \alpha \Delta \alpha^* \rangle J_1 + \langle \alpha^* \Delta \alpha \rangle (1 - J_1)] e^{i\psi_r} + \langle |\Delta \alpha|^2 \rangle \cos\psi_t (J_1 - J_2)\} e^{i\psi_r} \quad (11c)$$

$$J_1 = \langle \sin^2\theta \rangle, \quad J_2 = \langle \sin^4\theta \rangle. \quad (11d)$$

where the brackets at polarizabilities denote averaging over particles' sizes and the brackets in $J_{1,2}$ stand for averaging in θ .

One can see that for random orientation of particles in φ , the alternate and SHV configurations produce the same Z_{DR} but ρ_{hv} exhibits different values. The magnitude of ρ_{hv} depends on ψ_t that can be used to get more information on scattering media if radar can change ψ_t .

The left panel in Fig. 2 presents Z_{DR} for plate-like and column-like particles uniformly distributed in φ and flatter uniformly in θ from zero to maximal angle θ_o . It follows from the panel that if measured Z_{DR} exceeds 4 dB and there is evidence that particles have no preferable orientation in the horizontal plane, then particles have plate like shapes. To verify that particles have no preferable orientations in φ , one can analyze the azimuthal dependence of Z_{DR} if radar echo coverage is large enough. For networked radars, measurements from different radars can be used for that.

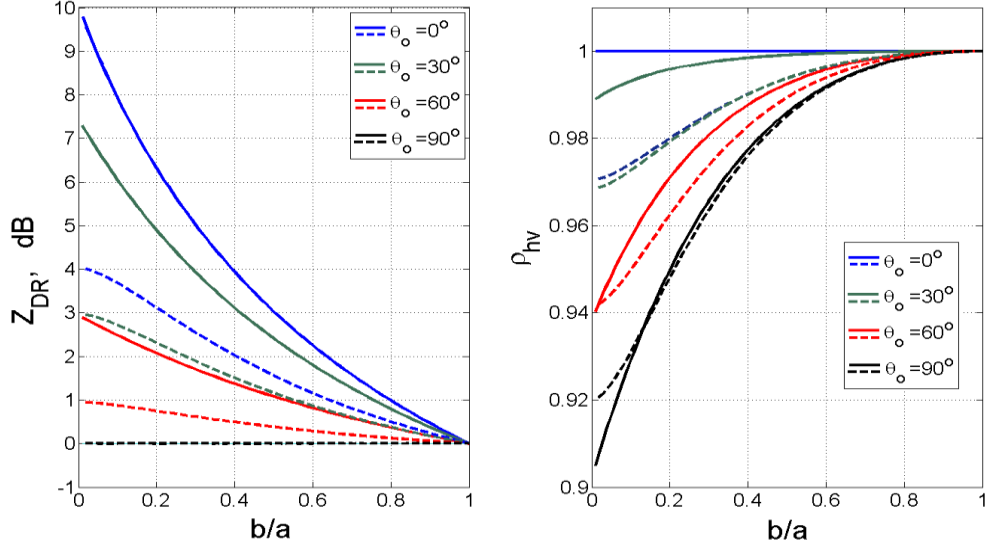


Fig. 2. (left) Z_{DR} and (right) ρ_{hv} for flattering ice cloud particles as functions of the aspect ratio b/a . The solid curves are for the plate-like particles and the dashed lines are for the needle-like ones. σ_θ is the maximal flatter angle in θ . Flattering is uniformly distributed in θ from 0 to θ_o ; the distribution in φ is uniform.

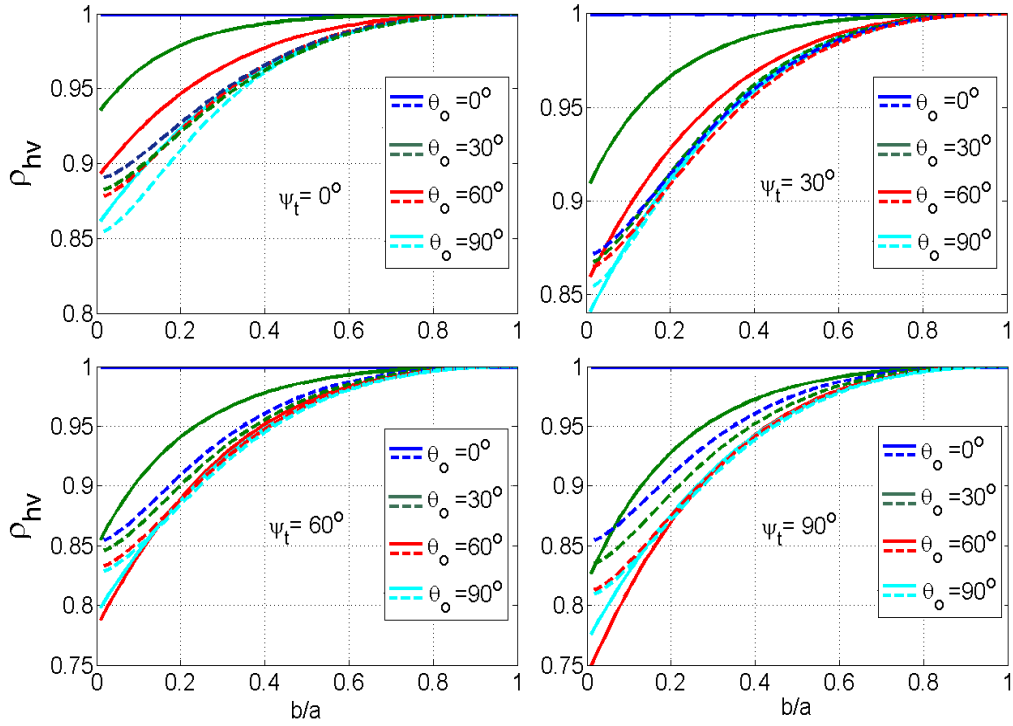


Fig. 3. Coefficients ρ_{hv} for the SHV configuration as a function of b/a for (the solid lines) plate-like and (dashed lines) column-like ice particles. ψ_t is the phase upon transmission, θ_o is the maximum flatter angle.

The correlation coefficients ρ_{hv} for the SHV configuration are depicted in Fig. 3 for different phase in transmit ψ_t . It is seen by comparing the right panel in Fig. 2 with Fig. 3 that depolarization degrades ρ_{hv} significantly.

3. Radar observations

Dual polarization radar observations in non-precipitation clouds were conducted with the 11-cm wavelength WSR-88D KOUN located in Norman, OK. The radar employs the sHV polarimetric configuration (Doviak et al. 2000, Zrníc et al.,

2006). Three cases of radar observations are presented in Fig. 4 in a form of vertical cross sections, i.e., RHIs. A ground clutter filter with the notch of $\pm 2 \text{ m s}^{-1}$ has been used to generate the RHIs. In Z_{DR} panels one can see large areas with $Z_{DR} > 5 \text{ dB}$ colored with black.

In panel (a) ground clutter residues can be seen within distances of 5 km whereas in panels (g, h) residues are seen up to 14 km with reflectivity less than -10 dBZ . The residues in panels (d) and (e) are negligible that is confirmed with the Doppler velocity field (not shown).

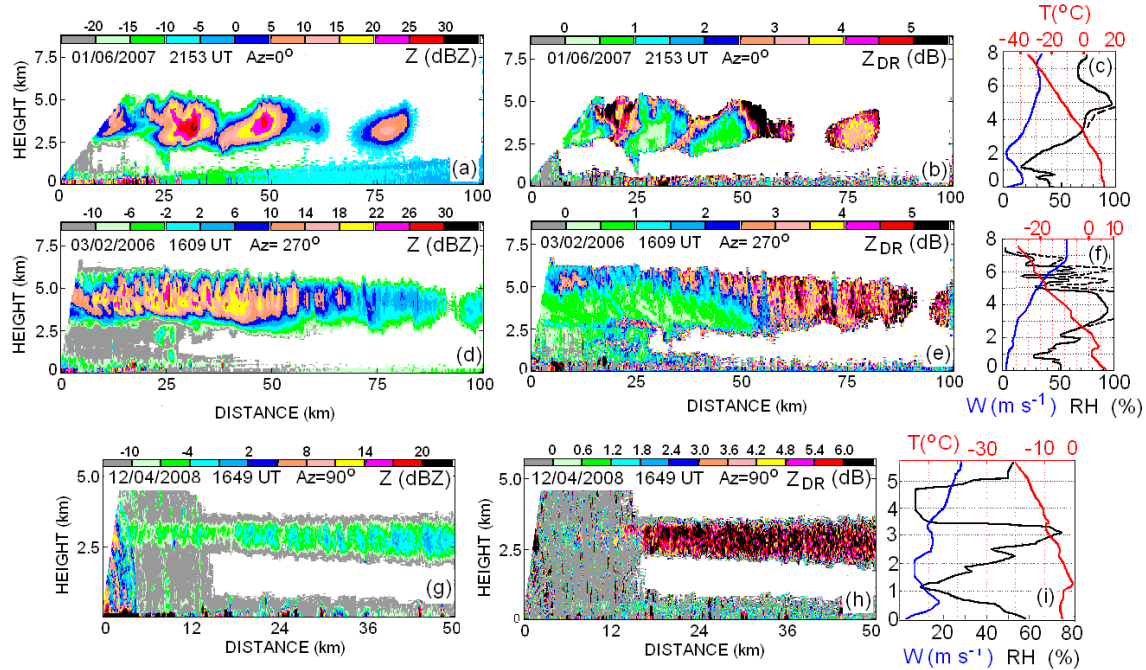


Fig. 4. Vertical cross sections of reflectivity and differential reflectivity on (the top row) January 6, 2007 at 2153, (the central row) March 2, 2006 at 1609, and (the bottom row) December 04, 2008 at 1649. The right panels depict profiles of temperature, T , wind speed, W , and relative humidity, RH , with respect to water (the solid black lines) and ice (the dash black lines) obtained from rawinsonde sounding at Norman, OK, (c): 01/07/2007 00UT, (f): 03/02/2006 1200UT, and (i): 12/05/2008 1200UT.

In calculations of Z_{DR} , the noise powers in the horizontal and vertical channels should be measured with high accuracy. They were obtained from areas beyond radar echoes. The conventional estimates of Z_{DR} have been compared also against the ones obtained via the correlation algorithm (Melnikov and Zrníc, 2007) which has no bias due to uncertainty in the noise levels. Both estimates show about the same areas with $Z_{DR} > 6 \text{ dB}$.

Radar was calibrated in Z_{DR} according to Zrníc et al. (2006) with accuracy about $\pm 0.1 \text{ dB}$.

To decrease statistical uncertainties of radar moments' estimations, the number of samples in collected data was 128 with 4 times oversampling in elevation and twice range oversampling which makes the equivalent number of samples 768 for a representation range gate. The standard deviations in reflectivity and Z_{DR} are shown in Fig. 5. For $\text{SNR} > -5 \text{ dB}$, the standard deviations are less than 1 dB which is sufficient to produce meaningful radar fields.

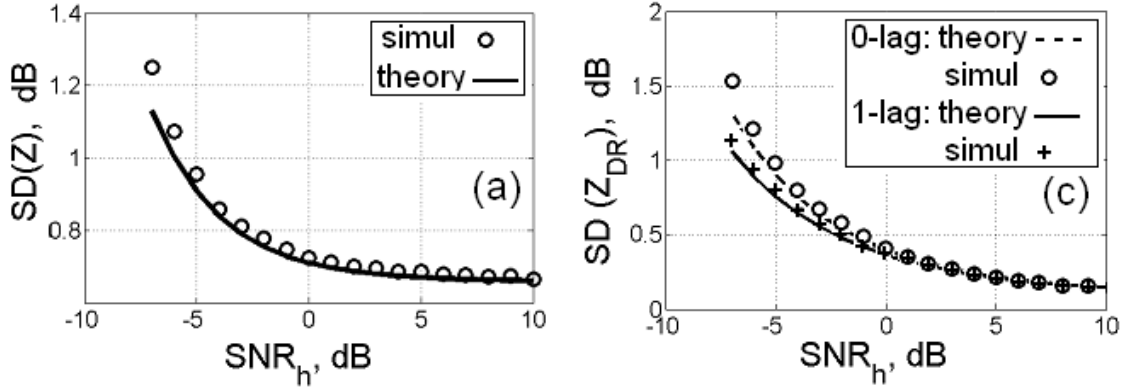


Fig. 5. The standard deviation of measured Z and Z_{DR} obtained from calculations (the lines) and signal simulations (the circles and pluses) for the 0-lag and 1-lag estimators. The number of averaged samples is 768.

In the Z_{DR} panels in Fig. 4(b, e), one can see quite large areas with $Z_{DR} > 4$ dB, i.e., observed Z_{DR} exceed the limit derived in the previous section for horizontally oriented solid ice columns. In these cases, spatial cloud structures exhibit strong influence of convection so that random orientation of particles in the horizontal plane is very likely. So we conclude that the areas with $Z_{DR} > 4$ dB in Fig. 4 (b, e) contain plate-like particle. In Fig. 4(h) the whole cloud volume contains particles with $Z_{DR} > 4$ dB and Z_{DR} exhibits no azimuthal dependence. So we can conclude that the particles have plate-like shapes.

Distributions of the measured Z_{DR} for $\text{SNR}_{h,v} > -5$ dB are presented in Fig. 6 for the two cases. For this SNR and the one-lag estimator, the standard deviation of Z_{DR} measurements is 0.65 dB. On 01/06/2007 (the left panel of Fig. 6), the data have been taken from a box with the following boundaries: range is from 52 to 56 km and heights are from 3.5 to 5 km. On 12/04/2008 (the right panel), the data were analyzed at distances beyond 20 km to avoid possible contamination from ground clutter residues. It is seen from Fig. 6 that the vast majority of Z_{DR} exceeds 4 dB. So these areas contain plate-like particles.

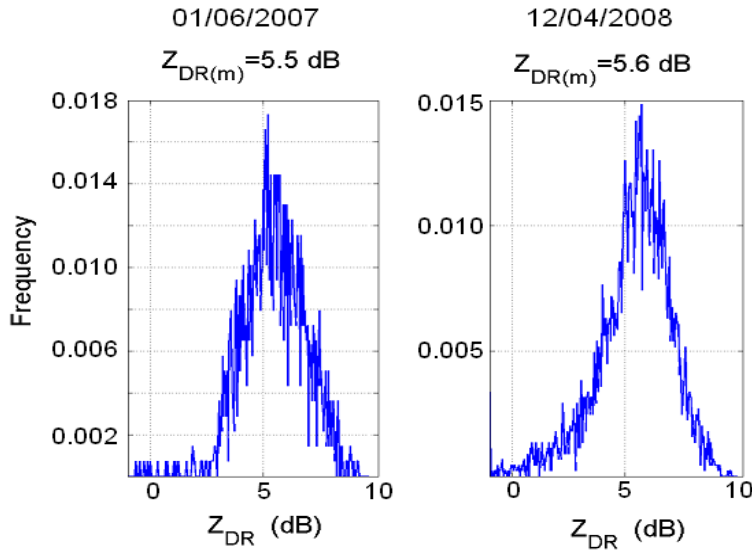


Fig. 6. Frequency of occurrence of Z_{DR} on (left) 01/06/2007 at 2153 UT and (right) 12/04/2008 at 1649 UT. $Z_{DR(m)}$ stands for the median value. Corresponding radar vertical cross sections are shown in Fig. 3 (b, h).

One more example of a large area with plate-like particles is shown in Fig. 7. The data were collected with WSR-88D KOUN in operational VCP#31 at elevation of 3.5° . One can see a large area of high Z_{DR} to the West - North-

west from the radar. Maximal Z_{DR} in the area reach 7.9 dB which is the maximal measurable value for the operational radar modes. The data presented in Figs. 5 and 6 have been collected with a “cloud” VCP that has no such a limitation.

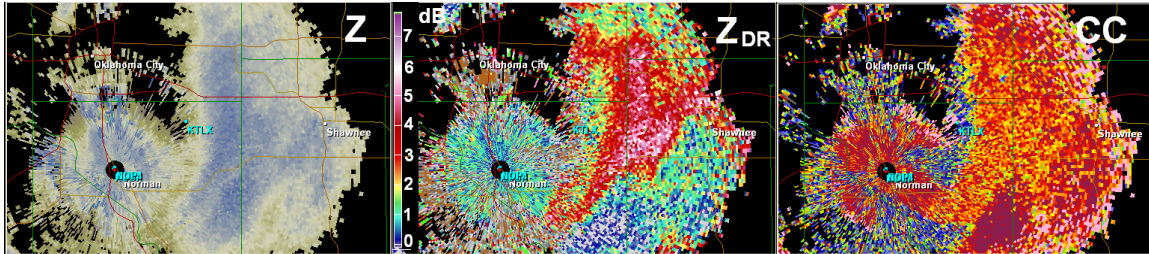


Fig. 7. Polarimetric fields collected with WSR-88D KOUN on 1 Feb. 2011 at 1948 Z. The elevation angle is 3.5° . CC stands for Correlation Coefficient, i.e., ρ_{hv} .

4. Conclusions

- Maximal Z_{DR} for the alternate radar polarimetric configuration for plate-like solid ice particles is 10.0 dB. This maximum is achieved at straight horizontal orientation of particles. For the SHV polarimetric configuration maximal Z_{DR} is 11.5 dB that is attained for aligned particles with the canting angle of about 10° .
- Column-like ice particles have maximal Z_{DR} of 6.4 dB for the alternate and SHV configurations. This value is achieved for horizontally oriented particles aligned along incident electromagnetic field. For randomly oriented particles in the horizontal plane, maximal Z_{DR} for column-like particles is 4.0 dB.
- In clouds with strong convective motions particles are randomly oriented in the horizontal plane and areas with $Z_{DR} > 4$ dB contain plate-like ice particles (Fig. 4(b, e)). In clouds without visible undulations (e.g., Fig. 4(h)), if Z_{DR} field does not exhibit an azimuthal dependence, areas with $Z_{DR} > 4$ dB contain plate-like ice particles.
- Additional information on particles' shapes can be obtained by analyzing the copolar correlation coefficients ρ_{hv} . In the SHV configuration, ρ_{hv} exhibits a dependence on the system differential phase upon transmission that can be used to obtain information on shapes and fluttering of particles.

References

- Bohren, C.F., and D.R. Huffman, 1983: *Absorption and Scattering of Light by Small Particles*, John Wiley and Son, San Diego, CA.
- Bringi, V. N., and V. Chandrasekar, 2001: *Polarimetric Doppler Weather Radar. Principles and Applications*. Cambridge University Press. 636 pp.
- Doviak, R.J., V. Bringi, A. Ryzhkov, A. Zahrai, D. Zrnica, 2000: Considerations for polarimetric upgrades to operational WSR-88D radars. *J. Atmos. Oceanic Technol.*, **17**, 257 – 278.
- Doviak, R. J. and D. S. Zrnica, 2006: *Doppler radar and weather observations*, 2nd ed., Dover Publications, 562 pp.
- Hall M.P.M., J.W.F. Goddard, and A.S.R. Murty, 1984: Identifications of hydrometeors and other targets by dual polarization radar. *Radio Sci.*, **19**, 132-140.
- Hogan, R.J., P. R. Field, A. J. Illingworth, R. J. Cotton and T.W. Choulaton, 2002: Properties of embedded convection in warm-frontal mixed-phase cloud from aircraft and polarimetric radar. *Q. J. R. Meteorol. Soc.*, **128**, pp. 451–476.
- Illingworth A.J., J.W.F. Goddard, and S.M. Cherry, 1997: Polarization radar studies of precipitation development in convective storms. *Q. J. R. Meteorol. Soc.*, **113**, 460-489.
- Kennedy, P. C., S. A. Rutledge, 2011: S-Band Dual-Polarization Radar Observations of Winter Storms. *J. Appl. Meteor. Climatol.*, **50**, 844–858.

- Matrosov, S.Y., 1991: Theoretical study of radar polarization parameters obtained from cirrus clouds, *J. Atmos. Sci.*, 48, 8, 1062–1069.
- Matrosov, S.Y., R. F. Reinking, R. A. Kropfli, and B. W. Bartram, 1996: Estimation of ice hydrometeor types and shapes from radar polarization measurements, *J. Atmos. Oceanic Technol.*, 13, 85–96.
- Melnikov, V.M., and D.S. Zrníc, 2007: Autocorrelation and cross-correlation estimators of polarimetric variables. *J. Atmos. Ocean. Technol.*, **24**, 1337-1350.
- Melnikov, V. M., D. S. Zrníc, R. J. Doviak, P. B. Chilson, D. B. Mechem, Y. Kogan, 2011: Prospects of the WSR-88D Radar for Cloud Studies. *J. Appl. Meteor. Climatol.*, **50**, 859–872.
- Vivekanandan, J., W. M. Adams, and V. N. Bringi, 1991: Rigorous approach to polarimetric radar modeling of hydrometeor orientation distributions, *J. Appl. Meteorol.*, 30, 1053–1063.
- Vivekanandan, J., V. N. Bringi, M. Hagen, and P. Meischner, 1994: Polarimetric radar studies of atmospheric ice particles,” *IEEE Trans. Geosci. Remote Sensing*, 32, 1-10.
- Zrníc D.S., V. M. Melnikov, and J. K. Carter, 2006: Calibrating differential reflectivity on the WSR-88D. *J. Atmos. Ocean. Technol.*, **23**, 944-951.